Research Square

Preprints are preliminary reports that have not undergone peer review.
They should not be considered conclusive, used to inform clinical practice,
or referenced by the media as validated information.

Year-Resolved Quasi-Static Time-Series Assessment of Photovoltaic Hosting Capacity in a 59-Bus 22 kV Egyptian Distribution Network Model

Karim Abouelenein

kareemali19990@gmail.com

Independent https://orcid.org/0009-0006-4639-8204

Research Article

Keywords: photovoltaic hosting capacity, quasi-static time-series, distribution network, Egypt, overvoltage, Monte Carlo

Posted Date: November 27th, 2026

DOI: https://doi.org/10.21203/rs.3.rs-11881914/v1

License: This work is licensed under a Creative Commons Attribution 4.0 International License.
Read Full License

Additional Declarations: The authors declare no competing interests.

Year-Resolved Quasi-Static Time-Series Assessment of Photovoltaic Hosting Capacity in a 59-Bus 22 kV Egyptian Distribution Network Model

Karim Abouelenein

Independent Researcher, Mansoura, Egypt

Email: kareemali19990@gmail.com

Abstract

A year-resolved quasi-static time-series (QSTS) assessment of the 59-bus, 22 kV Cairo distribution network model of [11] (peak load 50.34 MW) gives an overvoltage-limited photovoltaic (PV) hosting capacity (HC) of 165% of peak load (HC95 over 200 random placements, 1.02 p.u. substation setpoint, 95% bootstrap CI 150-189%). Each scenario uses 8760 hourly AC load flows with PVGIS-SARAH3 irradiance and a national-scale load shape built from Ember monthly demand and the EEHC peak-day curve; no feeder measurements were available. A snapshot at the year's lowest daytime load with peak PV output reproduces the level (160%), so a well-chosen snapshot is adequate on this network, while an arbitrary 25%-load snapshot (115%) is far too conservative and a 24 h mean day (215%) overestimates the HC. Overvoltage occurs on average in about 4 h per year, at 11:00-12:00 local time in spring (mostly April), and the full-year HC95 stays within 165-170% across all 19 simulated years (2005-2023). Sensitivities to tilt, load level, time alignment and substation setpoint are reported; thermal limits, whose ratings are not published, are examined only under assumed values. To the author's knowledge, this is the first year-resolved AC QSTS HC study of an Egyptian MV network model found in the literature searched. The results are conditional on the stated assumptions.

Keywords: photovoltaic hosting capacity; quasi-static time-series; distribution network; Egypt; overvoltage; Monte Carlo.

I. Introduction

Egypt is expanding grid-connected PV under its net-metering and small-scale PV connection rules, and distribution companies need to know how much PV their networks can absorb before voltage or loading limits are violated. This maximum is the hosting capacity (HC). Reviews conclude that HC depends on topology, loading, control, limits and on the method used, and so must be assessed for each network [1], [2].

Methods range from a single worst-case snapshot (typically high PV output with low load), through time-series simulation, to stochastic placement studies [2]-[4]. Quasi-static time-series (QSTS) simulation evaluates every hour and is the usual reference. The U.S. National Renewable Energy Laboratory compared snapshot and year-long QSTS HC on a real feeder and found the snapshot more conservative [5], and a recent open-source application to a developing-country grid exists [6]. How large the snapshot difference is depends on how the snapshot is built and on the feeder, so it has to be checked for each network.

Published Egyptian work on PV or DG integration is extensive but, as far as the literature searched here shows, is mainly deterministic, short-circuit-impedance-based, or optimization-based. Examples include voltage-profile impact studies on Egyptian networks [7], a PSS/E short-circuit-impedance and inverter-control method applied to part of an Egyptian network [8], hosting capacity maximization under uncertainty on the East Delta network [9], and optimization of compensators and voltage regulators on a rural Egyptian feeder [10]. A recent full AC time-series study exists for the Niger River-zone grid [6], and year-long QSTS HC methodology is documented in [5]. We found no full-year AC QSTS HC study for an Egyptian MV network.

This paper applies year-resolved QSTS to the 59-bus, 22 kV Cairo network model of [11], previously studied by the author with a single critical hour [18]. The method is not new; the contribution is its application and the findings for this network. Contributions: (i) a year-resolved (8760 h) AC QSTS overvoltage HC assessment with multi-year PVGIS irradiance and a load shape built from measured national aggregate data; (ii) a comparison of snapshot, 24 h and full-year HC on identical placement scenarios, including how the snapshot definition changes the answer; (iii) identification of the binding hours and months; (iv) a 19-year stability check and sensitivity to tilted PV, load level, time alignment and substation setpoint; and (v) an open, reproducible code and data package. A thermal-limit sensitivity analysis under assumed ratings is given separately in Section V.

II. Related Work

HC quantification methods are reviewed in [1] and [2]. The U.S. National Renewable Energy Laboratory documented QSTS HC methodology and metrics and compared them with snapshot results on a real feeder [5]. Stochastic HC with randomized placements was developed for LV networks in [3]. For Egypt, [7] assessed the impact of PV on voltage profiles of Egyptian networks, [8] proposed a short-circuit-impedance and inverter-control method using PSS/E on part of an Egyptian distribution network, [9] maximized DG hosting capacity under uncertainty on the practical East Delta network using a metaheuristic, and [10] maximized hosting capacity with compensators and regulators on the rural Egyptian Talla system. The Tala distribution network was also studied with harmonic analysis in [12]. The 59-bus Cairo network data used here come from [11].

What those studies do not report, as far as this search found, is a year-resolved AC QSTS HC with multi-year irradiance for an Egyptian MV network, or the hours and months that bind there. This is the gap addressed here. The method itself is not new.

III. Methodology

A. Network

The network model is a radial 22 kV substation network with 59 buses, 58 in-service branches and six normally open tie lines, built from the published branch data in the appendix of [11] (the data are as published in [11]; this paper does not claim access to utility records) and validated against the base-case losses and voltages published with those data: at 100% load the model gives total losses of 218.9 kW and a minimum voltage of 0.9865 p.u., matching the published values (validate_solver.py in the accompanying package). The same model was used in the author's earlier study [18]. Peak load is 50.344 MW. The substation bus is the slack with voltage setpoint 1.02 p.u. in the main case and 1.00 p.u. as a sensitivity. The upper voltage limit is 1.05 p.u.

B. QSTS solver

Hourly AC load flows use a vectorized backward/forward sweep for radial networks with constant-power loads, solving all time steps at once. The solver was checked against pandapower [13] on 40 random operating points spanning the load and PV range (maximum bus-voltage difference 2.7e-9 p.u.), and for ten random scenarios at a realistic snapshot hour it gives per-scenario HC values identical to pandapower on the 5% penetration grid (validate_solver.py in the accompanying package). Hours without PV output are not evaluated because voltage cannot exceed the slack value there.

C. PV model and irradiance

Hourly irradiance and temperature for Cairo (30.04 N, 31.24 E) come from PVGIS-SARAH3 for 2005-2023 [14]. In the main case, PV output per unit of rated power is computed from horizontal irradiance G as G/1000 x (1 - 0.004 (Tc - 25)) x 0.86, with cell temperature Tc = T2m + 0.031 G, unity power factor and a cap at 1.0. These coefficients are modeling assumptions. In the tilt sensitivity, G is replaced by the plane-of-array irradiance (beam + diffuse + reflected) that PVGIS returns for a 30-degree slope facing south, with the same temperature model. Local time is UTC+2 throughout (daylight saving ignored), and 29 February is removed.

D. Load model

No open measured hourly load series for Egypt, Cairo or any Egyptian feeder was found. The main load shape is therefore a national-scale composite: monthly demand factors from Ember monthly data for Egypt (mean of 2016-2025, per-day energy) multiplied by the diurnal curve of the EEHC peak day 2022/23 digitized from the EEHC annual report [15], [16], normalized so that the annual maximum is 1.0 (minimum 0.575). No weekly pattern is available, so weekly factors are set to 1. An earlier assumed shape (summer-evening peak, Jul/Aug maximum, Friday factor 0.92) is kept for comparison. The digitization is accurate to about 1% of peak and the shape is not a feeder measurement. Because the EEHC curve is a summer peak-day, it may overstate spring midday load, which is the critical period found here.

E. Placement scenarios and the HC metric

Each of 200 scenarios places 5-20 PV units at randomly drawn load buses with squared-uniform relative sizes, using the same random seeds as the author's earlier study [18]. Total PV capacity is expressed as a percentage of peak load (penetration) and varied on a 5% grid up to a 400% cap. For each scenario the HC is the largest penetration with no overvoltage in any evaluated hour. Monotonicity of violation in penetration, which allows bisection, was checked for the voltage limit (2019, 1.02 p.u.) on the full 5% grid for all 200 scenarios (test_monotone.py in the accompanying package). The population HC95 is the 5th percentile of per-scenario HC, so 95% of placements are violation-free, with a 95% bootstrap confidence interval (1000 resamples). Because many scenarios reach the cap, means are truncated and HC95 is the more reliable figure; where more than half of scenarios are capped (slack 1.00 p.u.), HC95 is a lower bound.

F. Methods compared

On identical scenarios the study compares: (1) a legacy snapshot at 25% of peak load with full PV output, the critical-hour practice of the author's earlier study [18]; because the lowest load in the national shape is 0.575 of peak, this snapshot lies below any load that actually occurs and is kept only to show the effect of an unrealistic snapshot; (2) a realistic snapshot: the lowest load during PV-producing hours of the year (0.575 of peak) combined with the highest PV output of the year (0.788 per unit); (3) a second realistic snapshot with the lowest load among hours at 90% or more of the peak PV output (0.677 of peak, same PV); (4) a 24 h mean day (hour-of-day averages of load and PV); (5) a 24 h worst day, the day with the largest net PV minus load; and (6) the full-year 8760 h QSTS. Snapshots (2) and (3) and the worst day (5) are selected from the full 8760 h series of the same year, so choosing them requires the annual series or equivalent annual data; they are realistic operating points, not a priori choices. The binding hours are the violating hours observed at the first violating level (HC + 5%), pooled over scenarios.

IV. Results

A. Snapshot versus 24 h versus full year

Table I. Overvoltage-limited HC95 (% of peak load), national load shape, 2019, substation 1.02 p.u., 200 scenarios. CI bounds are bootstrap percentiles rounded to the nearest integer.

Method	HC95	95% CI	Capped share
Snapshot, 25% load, full PV (legacy)	115	105-130	6%
Snapshot, lowest daytime load, peak PV	160	140-180	25%
Snapshot, lowest load at high PV, peak PV	165	145-190	27%
24 h mean day	215	190-240	54%
24 h worst day	165	150-185	27%
Full year, 8760 h	165	150-189	27%

The full-year QSTS gives an HC95 of 165% of peak load (95% CI 150-189%). The result depends strongly on how the snapshot is defined (Table I, Fig. 1). The legacy snapshot at 25% load gives 115%, about 30% below the full year, but that snapshot assumes a load that never occurs in the national shape and it should not be read as a typical snapshot result. A snapshot built from the lowest daytime load and the peak PV output gives 160% (CI 140-180%), and the variant using the lowest load among high-PV hours gives 165%. Both are within one 5% grid step of the full year, and the first one ranks placements almost identically (correlation 0.998; legacy snapshot 0.93). Per scenario, the lowest-daytime-load snapshot equals the full-year HC in 28% of the scenarios and lies within one grid step in 52% (mean absolute difference 6.8 percentage points), the high-PV variant lies within one grid step in all 200 scenarios (equal in 56%, mean absolute difference 2.2 percentage points), and the legacy 25%-load snapshot lies within one step in only 6%. On this network and load shape, a carefully chosen snapshot therefore reproduces the full-year HC95 level; what it cannot do is show when the violations occur or confirm that the chosen load-PV pair is the right one without the annual series. The 24 h mean day overestimates HC at 215% because averaging removes the clear-sky peaks. The worst day matches the full year (165% against 165%), but identifying it requires the annual series (2019-04-22 in 2019). At a 1.00 p.u. substation setpoint the HC95 values are 259% (realistic snapshot) and 264% (full year); 72% of scenarios reach the 400% cap, so the full-year value is a lower bound.

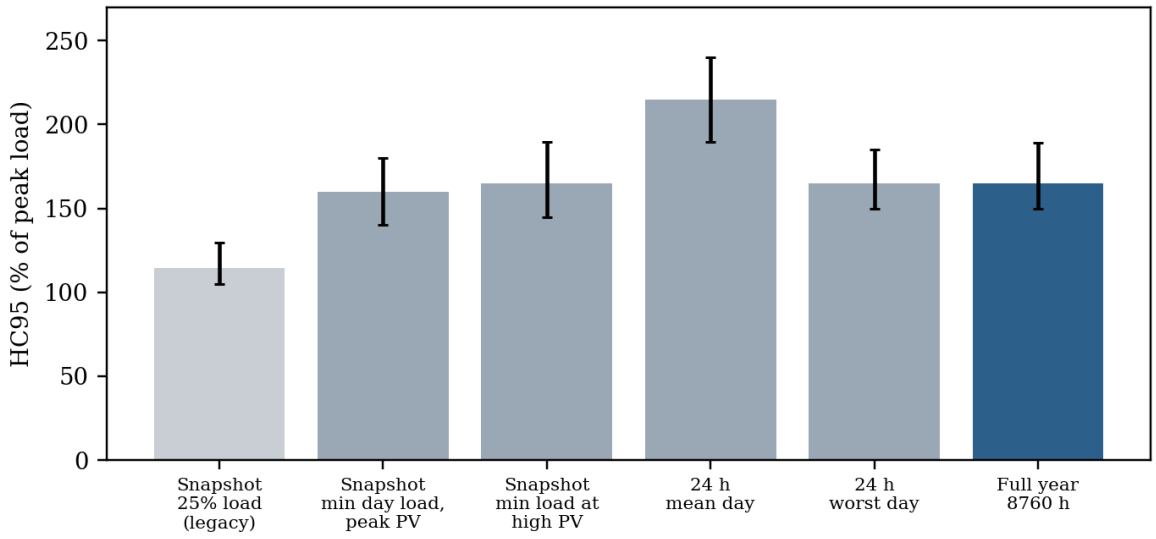

Fig. 1. HC95 by method, national load shape, 2019, 1.02 p.u. (error bars: 95% bootstrap CI).

With the earlier assumed load shape the same comparison gives a full-year HC95 of 160% and a realistic snapshot of 154% (lowest daytime load 0.32 of peak), so the conclusion that a realistic snapshot is close to the full year does not depend on the load shape used.

B. Binding hours and months

At the first violating penetration, overvoltage occurs on average in 4.1 h per year (median 4 h; 146 scenarios not capped). The violating hours are concentrated at 11:00-12:00 local time (1.61 and 2.45 violating hours per scenario at 11 and 12 h) and in the spring months, with 3.50 per scenario in April and 0.55 in May, and none in summer (Fig. 2). Violations occur when clear-sky irradiance is high, temperatures are moderate (higher module efficiency) and the load is not at its summer maximum, not when the load is lowest.

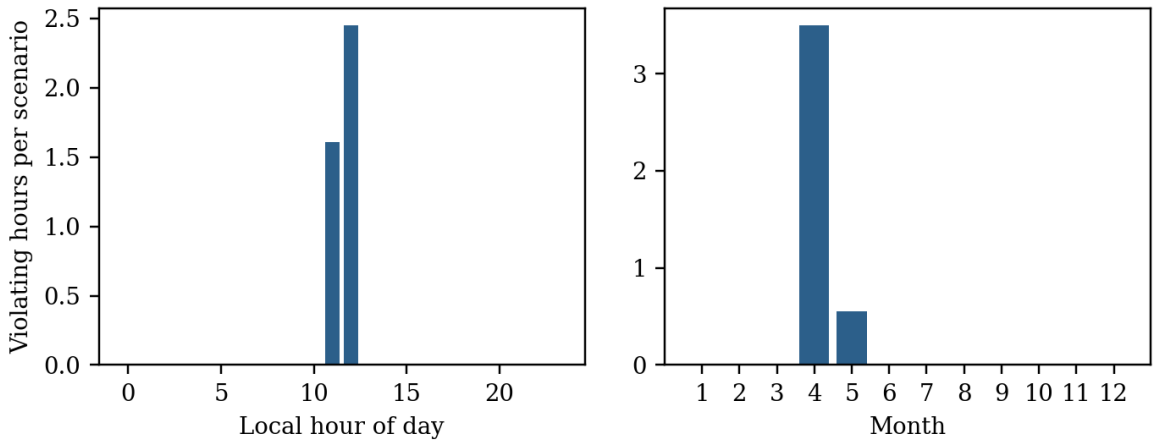

Fig. 2. Overvoltage violating hours per scenario at the first violating penetration, by hour and month (national load shape, 2019).

C. Year-to-year stability (all 19 years)

Table II. Overvoltage-limited HC95 (% of peak load) for each PVGIS year 2005-2023, national shape, 1.02 p.u., 200 scenarios. HC95 values are interpolated between grid points and rounded to the nearest 5% step.

Year	Full-year HC95	Realistic snapshot HC95	Worst day
2005	165	160	2005-04-25
2006	165	165	2006-03-29
2007	170	160	2007-04-30
2008	165	160	2008-04-30
2009	165	160	2009-04-27
2010	170	165	2010-04-12
2011	170	160	2011-04-25
2012	170	160	2012-03-30
2013	165	165	2013-04-22
2014	170	165	2014-04-27
2015	165	160	2015-04-24
2016	170	160	2016-03-30
2017	165	165	2017-04-25
2018	170	165	2018-04-23
2019	165	160	2019-04-22
2020	170	165	2020-04-29
2021	170	160	2021-04-11
2022	170	165	2022-03-26
2023	170	165	2023-04-30

All 19 years of the PVGIS record were simulated. The full-year HC95 lies between 165% and 170% in every year, a spread of 5 percentage points (at most one 5% grid step), and the realistic snapshot HC95 lies between 160% and 165%. The worst day falls in late March or April in every year (Table II). One representative year is therefore sufficient for this network.

D. Time alignment

The EEHC curve is a peak day in daylight-saving time while PVGIS is in UTC. Shifting the load by -1, 0 and +1 h relative to PV gives full-year HC95 of 165%, 165% and 170%, so the alignment ambiguity changes the result by at most one grid step. The national shape has higher spring midday load than the assumed shape (about 0.69 against 0.51 of peak at 11-12 h in March-April). If the true feeder midday spring load is lower than the national shape, the true HC would be lower than reported; the national curve therefore does not provide a safe upper bound.

E. Tilted PV

Using PVGIS plane-of-array irradiance for a 30-degree south tilt instead of horizontal irradiance raises 2019 annual PV energy by 10% (capacity factor 19.4% to 21.3%). The voltage-limited full-year HC95 is 165% (95% CI 150-189%) for horizontal irradiance and 155% (CI 140-179%) for the tilted plane, a difference of -10 percentage points. A paired bootstrap on the same 200 placements gives a 95% interval of -15 to -10 percentage points for that difference, so the reduction is consistent across placements but small: the point estimate is two 5% grid steps (the interval spans at most three), and the separate confidence intervals of the two estimates overlap. Horizontal irradiance therefore slightly overstates overvoltage-limited HC. Tracking arrays and east-west layouts were not tested.

F. Load level (+-20%) and substation setpoint

Scaling the national load shape by 0.8 and 1.2 gives voltage-limited full-year HC95 of 160% and 170%, against 165% at 1.0 (Table III). Penetration is still expressed relative to the nominal 50.34 MW peak. Within 20% load uncertainty the voltage-limited HC95 moves by up to 5 percentage points, so the result is not sensitive to the level of the load. It is far more sensitive to the substation setpoint: 165% at 1.02 p.u. against a lower bound of 264% at 1.00 p.u.

V. Thermal-Limit Sensitivity Analysis (assumed ratings)

Conductor and transformer ratings are not published for this network (the line data in [11] give only resistance and reactance), so the results in this section are a sensitivity analysis under explicit assumptions and are not findings about the real network. Line limits: each branch rating is the larger of 1.25 times its current at 100% load with no PV, and a uniform minimum ampacity of 200 A or 300 A (assumed values, not from the network owner). Branch ratings then range from 200 to 385 A (200 A case) and 300 to 385 A (300 A case); the highest no-PV peak branch current is 308 A. Substation limit: apparent power at the slack, in either direction (so reverse flow is included), may not exceed 1.0 or 1.25 times the no-PV peak apparent power (55.0 MVA). A combined case enforces voltage, the 300 A line limit and the 1.25x substation limit together. I2R heating and ambient derating are not modeled.

Table III. Full-year HC95 (% of peak load) by constraint, PV model and load level; national load shape, 2019, 1.02 p.u., 200 scenarios. Thermal ratings are assumptions. With load x1.2 the no-PV peak apparent power already exceeds 1.0x the nominal-peak substation rating, so that entry is 0.

Constraint	Horizontal PV	30 deg tilt PV	Horizontal, load x0.8	Horizontal, load x1.2
Voltage only (1.05 p.u.)	165	155	160	170
Line limit, 200 A min.	40	40	40	45
Line limit, 300 A min.	60	55	60	60
Substation 1.0x peak S	220	205	205	0
Substation 1.25x peak S	260	240	240	275
Combined V + 300 A + 1.25x	60	55	60	60

Under the assumed ratings the line limit binds well before overvoltage (Table III, Fig. 3): with a 300 A minimum ampacity the full-year HC95 is 60% of peak load (CI 55-65%), and 40% with 200 A, compared with 165% for voltage alone. The substation limit alone allows 220% (1.0x) or 260% (1.25x) because of reverse power flow. With all three limits applied, the combined HC95 equals the line-limited value.

The binding branches were analyzed at the first violating penetration of the 300 A case. Across the 200 scenarios, 271 branch violations occurred (1.36 per scenario). 89% of the violated branches are rated at the 300 A floor, meaning that 1.25 times their own no-PV peak current is below 300 A; their median no-PV peak current is 129 A. In every violated branch the PV connected downstream (19.1 MW median) exceeds the downstream peak load (4.5 MW median), so the branch carries net export, and its highest current (308 A median) just exceeds the 300 A floor. Only 18% of the violations are on branches that connect directly to the substation bus. The thermal HC is therefore set mainly by the assumed uniform minimum ampacity applied to lightly loaded branches that carry the exported PV power of several buses, not by a property established for the real cables. With real ratings the binding limit and the HC could be very different, in either direction.

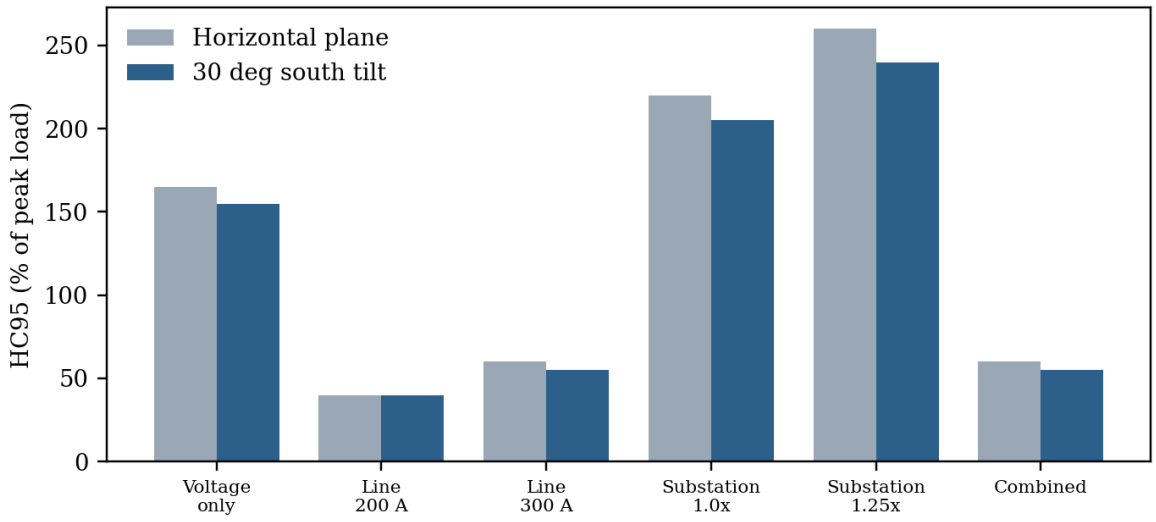

Fig. 3. Full-year HC95 by constraint for horizontal and 30-degree tilted PV (thermal ratings assumed).

VI. Discussion

The overvoltage-limited full-year HC95 of the 59-bus network model is 165% of peak load at a 1.02 p.u. setpoint. The critical period is not the summer and not the lowest-load hour; it is a few spring midday hours,

in late March and April, when PV output is high, temperature is moderate and the load shape is below its summer peak. A snapshot at the right combination of load and PV reproduces the HC95 level on this network (160% against 165%), but the 25%-load snapshot used in earlier work [18] is too conservative (115%), and a mean-day profile overestimates the HC (215%). The practical value of the year-resolved run is therefore to identify the binding season and hours, to confirm that the chosen snapshot is representative, and to show that the result is stable across 19 years of irradiance. The magnitude of any snapshot difference depends on the load shape and on the network and should be checked for each case.

Compared with the Egyptian studies cited above, this work does not propose a new algorithm or control; it supplies a reproducible year-resolved reference for a published Egyptian MV network model. The thermal sensitivity shows that conclusions based on overvoltage alone could be optimistic for networks with modest conductor ratings, but whether this is true for the real network depends on ratings that were not available.

Mitigation (Volt-Var or Volt-Watt inverter control, on-load tap changer settings, storage) was not simulated here. Egyptian studies have reported HC improvement from smart-inverter and reactive-power control on other networks [8], [17]; applying such controls inside the year-resolved framework is a direct next step.

VII. Limitations

- The load is a national-scale composite from monthly Ember data and one digitized EEHC peak-day curve. It is not a measurement of this feeder or of any Egyptian substation. Feeder loads are typically peakier and more residential. Real hourly substation data would change absolute values, especially the spring midday load that governs the result.
- The network is a published model from [11], not utility-supplied data, and no field measurements were used for validation.
- Thermal ratings and substation capacity are assumptions, not network data. The thermal HC values are conditional on them and must not be read as properties of the real network.
- Only voltage and loading are evaluated; voltage unbalance, flicker, harmonics, protection, short-circuit level and dynamic stability are not.
- PV is lumped at MV buses at unity power factor with a simple temperature model and a fixed derate. Rooftop PV on LV feeders is not represented. Cloud transients within an hour are not captured by hourly resolution.
- Local time is UTC+2 with daylight saving ignored; the +-1 h alignment sensitivity was tested only for the national shape.
- Placement scenarios are random, with 200 scenarios per setting. Many scenarios reach the 400% cap at 1.00 p.u., so HC95 is a lower bound there.
- No mitigation (Volt-Var, tap changers, storage) is modeled, so the HC values are for passive unity-power-factor PV.
- The literature search for prior work used web searches and abstracts, not a full database search of Scopus or Web of Science. The claim that no prior Egyptian year-resolved AC QSTS HC study exists is limited to what this search found.

VIII. Conclusion

A year-resolved AC QSTS assessment of the 59-bus, 22 kV Cairo network model gives an overvoltage-limited PV hosting capacity of 165% of peak load (HC95, 1.02 p.u., 95% CI 150-189%). A snapshot built from the lowest daytime load and peak PV gives 160%, within one grid step, while an arbitrary 25%-load snapshot gives 115% and a 24 h mean day gives 215%. Violations are confined to a few hours around noon in

spring and the result is stable across all 19 irradiance years (165-170%), changes by 10 percentage points (two grid steps) under a 30-degree tilt and by up to 5 percentage points under +-20% load, and is far more sensitive to the substation voltage setpoint. Thermal limits, examined only under assumed ratings, could reduce the HC well below the overvoltage limit. Measured feeder load and conductor ratings from a distribution company are the most valuable next step, followed by Volt-Var control within the same framework.

Data availability and reproducibility

The code (vectorized QSTS engine, experiments, thermal and tilt extensions, and the pandapower validation script and the monotonicity check), the PVGIS irradiance files, the final 8760-h load-shape file and all result tables are included in the accompanying package; seeds are deterministic. Network data are republished from the appendix of [11]. Ember data are CC BY 4.0; the EEHC curve is digitized from the cited report and the report itself is not redistributed; PVGIS data are used under the European Commission JRC PVGIS terms.

Acknowledgment and AI disclosure

A generative AI assistant was used under the author's direction to help write the code, produce the figures and draft the text. The author directed the study, checked the results by re-running the code, and is responsible for the content.

References

[1] E. Mulenga, M. Bollen, and N. Etherden, "A review of hosting capacity quantification methods for photovoltaics in low-voltage distribution grids," Int. J. Electr. Power Energy Syst., 2019. doi:10.1016/j.ijepes.2019.105445

[2] S. Fatima, V. Puvi, and M. Lehtonen, "Review on the PV hosting capacity in distribution networks," Energies, vol. 13, no. 18, 4756, 2020. doi:10.3390/en13184756

[3] M. Deakin, C. Crozier, D. Apostolopoulou, T. Morstyn, and M. McCulloch, "Stochastic hosting capacity in LV distribution networks," arXiv:1902.08780, 2019. https://arxiv.org/abs/1902.08780

[4] A. Koirala, T. Van Acker, R. D'Hulst, and D. Van Hertem, "Hosting capacity of photovoltaic systems in low voltage distribution systems: a benchmark of deterministic and stochastic approaches," Renew. Sustain. Energy Rev., 2022. doi:10.1016/j.rser.2021.111899

[5] A. K. Jain, K. Horowitz, F. Ding, N. Gensollen, B. Mather, and B. Palmintier, "Quasi-static time-series PV hosting capacity methodology and metrics," in Proc. IEEE Innovative Smart Grid Technologies Conf. (ISGT), Washington, DC, USA, 2019. doi:10.1109/ISGT.2019.8791569; preprint NREL/CP-5D00-72284. https://docs.nlr.gov/docs/fy19osti/72284.pdf

[6] H. A. Halarou, Y. Moumouni, B. A. Latif, A. M. Falmata, A. O. Fati, and M. Saidou, "A full AC time-series analysis of photovoltaic hosting capacity in Niger's grid," Energy Sci. Eng., vol. 14, no. 4, pp. 1952-1964, 2026. doi:10.1002/ese3.70456

[7] A. Mostafa, M. Kamh, K. Youssef, and M. Abdelrahman, "Assessment of photovoltaic penetration impact on voltage profile for distribution networks in Egypt," Proc. MEPCON, 2021. doi:10.1109/MEPCON50283.2021.9686195

[8] S. M. Sadek, A. A. Hassan, F. H. Fahmy, A. A. El-Deib, and H. K. M. Youssef, "Photovoltaic hosting capacity assessment in distribution networks," J. Electr. Syst. Inf. Technol., vol. 12, art. 102, 2025. doi:10.1186/s43067-025-00296-9

[9] A. Nazih, A. A. Abou El-Ela, and E. S. Ali, "Distributed generators hosting capacity maximisation under uncertainty: practical Egyptian network study," Aust. J. Electr. Electron. Eng., 2025. doi:10.1080/1448837x.2025.2568786

[10] A. M. Mahmoud, S. H. E. Abdel Aleem, A. Y. Abdelaziz, and M. Ezzat, "Towards maximizing hosting capacity by optimal planning of active and reactive power compensators and voltage regulators: case study," Sustainability, vol. 14, no. 20, 13299, 2022. doi:10.3390/su142013299

[11] Z. M. Ali, S. A. Abdel Aleem, F. Aldawsari, and Z. M. Zenhom, "Coordinated integration of renewables, STATCOMs, and V2G for hosting capacity improvement under uncertainty," Sci. Rep., 2026. doi:10.1038/s41598-026-57051-x

[12] E. S. Ali, A. A. Abou El-Ela, A. A. Mubarak, A. Nazih, and R. El-Sehiemy, "Optimal hosting capacity of photovoltaic sources for Tala distribution network with harmonic analysis," Proc. 26th Int. Middle East Power Syst. Conf. (MEPCON), 2025, pp. 1-7. doi:10.1109/MEPCON66918.2026.11360273

[13] L. Thurner et al., "pandapower: an open-source Python tool for convenient modeling, analysis, and optimization of electric power systems," IEEE Trans. Power Syst., vol. 33, no. 6, 2018. doi:10.1109/TPWRS.2018.2829021

[14] European Commission Joint Research Centre, "Photovoltaic Geographical Information System (PVGIS), PVGIS-SARAH3 hourly series," https://re.jrc.ec.europa.eu/pvg_tools/en/ (data retrieved November 2026).

[15] Ember, "Monthly Electricity Data," CC BY 4.0. https://ember-energy.org/data/monthly-electricity-data/

[16] Egyptian Electricity Holding Company, "Annual Report 2023/2024," https://www.eehc.gov.eg/CMSEehc/Files/AnnualReport2024En.pdf

[17] I. Hamdan, A. Alfouly, and M. A. Ismeil, "Hosting capacity enhancement for photovoltaic systems at various conditions based on Volt-Var control," Proc. MEPCON, 2022. doi:10.1109/MEPCON55441.2022.10021815

[18] K. Abouelenein, "Stochastic overvoltage-limited hosting capacity assessment of photovoltaic generation in an Egyptian medium-voltage substation network," submitted for publication, 2026.

Supplementary Files

This is a list of supplementary files associated with this preprint. Click to download.

- 2paper2packagev7fcdd61e21433947a.zip